Capacitance of a plate capacitor with one band-limited fractal rough surface

N.C. Bruce and A. García-Valenzuela
Centro de Ciencias Aplicadas y Desarrollo Tecnológico, Universidad Nacional Autónoma de México
Apartado Postal 70-186, 04510 México, D.F.

Recibido el 30 de marzo de 2007; aceptado el 20 de junio de 2007

The problem of the capacitance between a band-limited, zero-mean, fractal shaped-rough surface and a plane electrode is investigated. Five parameters are required to define the rough surface: σ, the rms height, D ($1 < D < 2$), the fractal dimension of the roughness; K_0, the fundamental spatial frequency; b ($b > 1$), the spatial frequency scaling parameter; and N, the number of spatial frequency components in the surface structure. We find that the graph of inverse capacitance against nearest electrode separation depends on σ and D, whereas it is nearly independent of K_0, b, and N for $N > 4$. The numerical results also indicate that the surface roughness can be interpreted as an equivalent dielectric film with an effective dielectric constant and effective thickness for surprisingly small minimum electrode separations. Our findings in this paper can be used to complement established techniques for the experimental determination of the statistical parameters of the surface roughness of conducting surfaces.

Keywords: Capacitance; fractal surfaces; capacitance microscopy.

Se investiga numéricamente el problema de la capacitancia entre una superficie rugosa con rugosidad fractal y una superficie lisa. Se requieren cinco parámetros para definir la rugosidad: σ, la altura rms; D ($1 < D < 2$), la dimensión fractal de la rugosidad; K_0, la frecuencia espacial fundamental; b ($b > 1$), el parámetro de escalamiento de la frecuencia espacial; y N, el número de componentes de frecuencia espacial en la superficie. Se encuentra que el inverso de la capacitancia contra la separación mínima entre los electrodos depende de σ y D, mientras que es independiente de K_0, b, y N para $N > 4$. Los resultados numéricos indican que la rugosidad superficial se puede interpretar como una película dieléctrica equivalente con una constante dieléctrica equivalente y grosor efectivo. Los resultados presentados en este artículo se pueden utilizar para complementar técnicas conocidas para la medición experimental de las propiedades estadísticas de la rugosidad superficial de superficies conductoras.

Descriptores: Capacitancia; superficies fractales; microscopia capacitiva.

PACS: 84.32.Tt; 84.37.+q

1. Introduction

There has been a great deal of interest recently in the measurement of rough surfaces using capacitance probes. Results have been presented for the capacitance between a plane or pointer probe electrode and deterministic (cosine or rectangular surface shape) conducting surfaces [1-10]. Recently, we presented a study of the capacitance obtained between a known probe electrode (which could be planar or with an array of pointers) and a random rough surface with Gaussian height statistics and a Gaussian correlation function [11]. In that work it was shown that the capacitance obtained with the planar probe electrode depended only on the height statistics and not the correlation statistics of the Gaussian rough surface, but that measurement with an electrode with a series of pointers gave information about the correlation function.

However, in practical situations, rough surfaces do not have Gaussian statistics; in general, rough surfaces are described by fractal functions [12]. In this paper, we study the simplest problem involving a rough surface with fractal statistics, that is, the capacitance of a parallel plate capacitor with one rough electrode. We report the results of a numerical study, assuming a rough surface described by a band-limited fractal. We require the use of a band-limited function because the numerical method we use to calculate the capacitance becomes unstable and inaccurate for high spatial frequencies ($\nu \gg 2D_0$ where ν is the spatial frequency and D_0 is a standard separation between the mean plane of the rough electrode and the plane of the flat electrode and is the scaling parameter for this problem) [6]. We study the two-dimensional problem due to the limitations of the numerical calculations for the full 3D problem.

2. Theory

The band-limited fractal function used to describe the rough surface height distribution, $h(x)$, is the following [13]:

$$h(x) = \sigma\, C \sum_{n=0}^{N-1} (D-1)^n \sin(K_0 b^n x + \phi_n), \tag{1}$$

where σ is the rms height, C is a normalizing factor for the rms height,

$$C = \left(\frac{2D(2-D)}{\left(1-(D-1)^{2N}\right)} \right)^{1/2}, \tag{2}$$

D ($1 < D < 2$) is the fractal dimension of roughness, K_0 is the fundamental spatial frequency, b ($b > 1$) is the spatial frequency scaling parameter, N is the number of spatial frequency components in the surface structure, and ϕ_n are random phases which give the different realizations of surfaces with the same fractal structure. Another important parameter for rough surfaces is the correlation length, τ_c, which is obtained from the correlation function $\rho(\tau)$:

$$\rho(\tau) = \frac{\langle h(x)\, h(x+\tau)\rangle}{\langle h^2(x)\rangle} = \frac{\left(1-(D-1)^2\right)}{\left(1-(D-1)^{2N}\right)} \sum_{n=0}^{N-1} (D-1)^{2n} \cos\left(K_0 b^n \tau\right), \quad (3)$$

where $\langle\rangle$ means the ensemble average, and the correlation length $\tau = \tau_c$ is found when $\rho(\tau) = \mathrm{e}^{-1}$. Figure 1 shows examples of rough surfaces generated with Eq. (1) and the associated parameters. It can be seen that for smaller values of D the rough surface is close to a sinusoidal shape, and as this parameter increases, the roughness increases and the surface finally looks nothing like a sinusoidal surface. For comparison, a surface with Gaussian statistics (height statistics and a Gaussian correlation function) is also shown in Fig. 1.

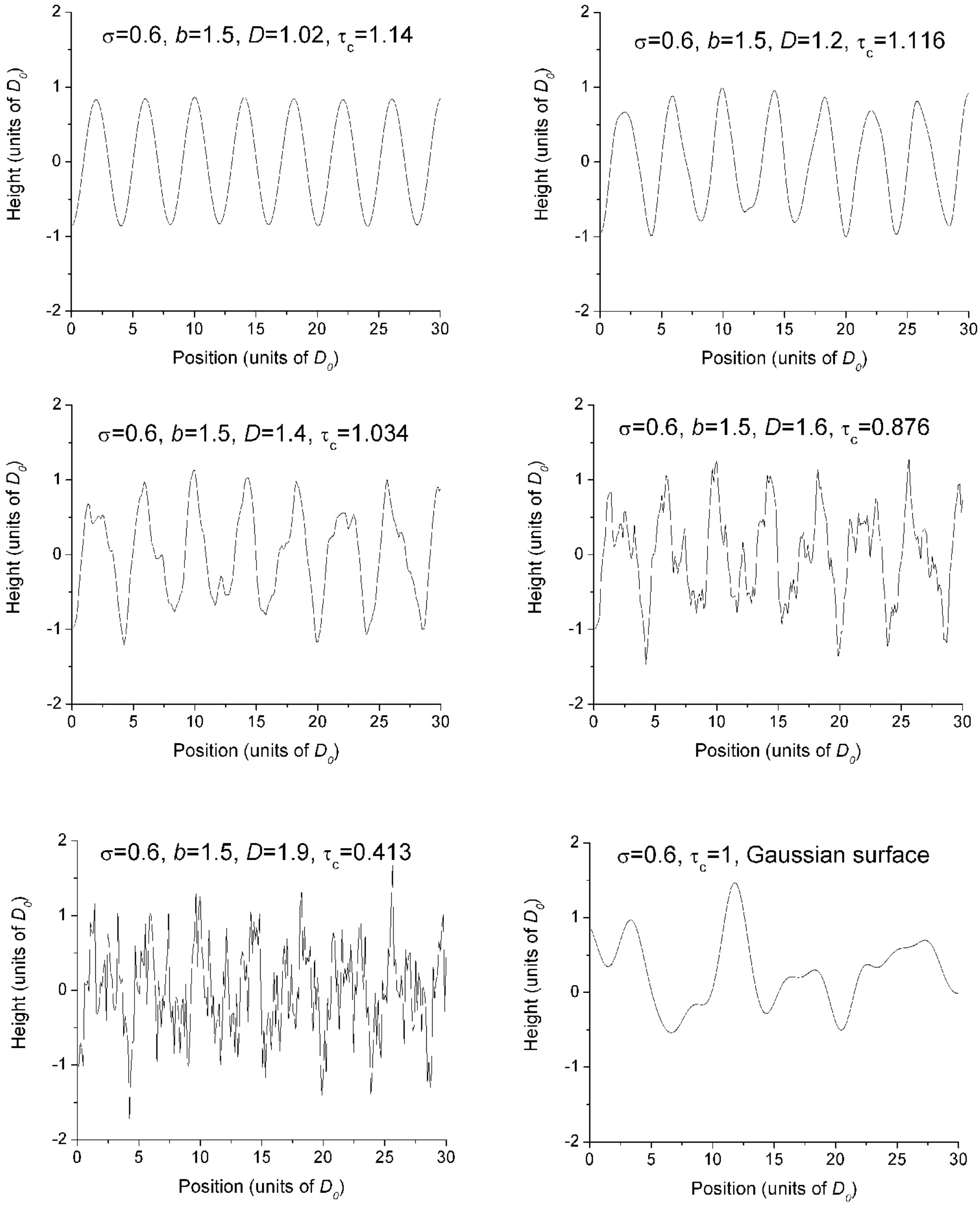

FIGURE 1. Examples of the band-limited fractal rough surface profiles and the parameters of the surfaces. Also shown for comparison is a Gaussian random rough surface with the same standard deviation of height and a correlation length comparable with the band-limited fractal surfaces.

The electric potential φ satisfies the Laplace equation

$$\nabla^2\varphi(r) = 0. \quad (4)$$

We can use Green's theorem to obtain the integral equation

$$\oint_{DR}\left(G(r-r')\frac{\partial\varphi(r)}{\partial n} - \varphi(r)\frac{\partial G(r-r')}{\partial n}\right)\mathrm{d}s = \begin{cases}\varphi(r') \text{ if } r' \in R \\ 0 \text{ if } r' \notin R\end{cases}, \quad (5)$$

where $G()$ is the Green function for this problem

$$G(r-r') = -\frac{1}{2\pi}\ln(|r-r'|),$$

n is the normal to the surface in the direction towards the volume R which is surrounded by the surface *DR*, and $\partial/\partial n = n\cdot\nabla$. Taking the point r' to be (i) infinitesimally below the plane probe surface (denoted by subscript a in the following equations) and (ii) infinitesimally above the rough test surface (denoted by subscript b) (see Fig. 2), we obtain the two equations [6]

$$\int_{-\infty}^{\infty}\left(U_b\frac{\partial G_{ba}}{\partial N} - G_{ba}B(x)\right)\mathrm{d}x - \int_{-\infty}^{\infty}\left(U_a\frac{\partial G_{aa}}{\partial y} - G_{aa}A(x)\right)\mathrm{d}x = 0$$

$$\int_{-\infty}^{\infty}\left(U_b\frac{\partial G_{bb}}{\partial N} - G_{bb}B(x)\right)\mathrm{d}x - \int_{-\infty}^{\infty}\left(U_a\frac{\partial G_{ab}}{\partial y} - G_{ab}A(x)\right)\mathrm{d}x = 0, \quad (6)$$

where the subscripts to the Green function indicate the source and field points of the field, for example, G_{ab} is the field at a point on surface b due to a unit source on surface a, $N$is the normal to the rough surface and the normal to the flat surface is in the direction of the y-axis. $A(x)$ and $B(x)$ are the charge densities on the top and bottom surfaces, respectively, normalized by the free space permittivity constant $\varepsilon_0 = 8.854\times10^{-12}C^2/N\,m^2$. Equations (6) are discretized, converted to matrix equations and solved in a computer to find $A(x)$ and $B(x)$. The normalized capacitance per unit length is then given by

$$C_N = \frac{1}{L}\int_0^L A(x)\ \mathrm{d}x = \frac{1}{L}\int_0^L B(x)\ \mathrm{d}x. \quad (7)$$

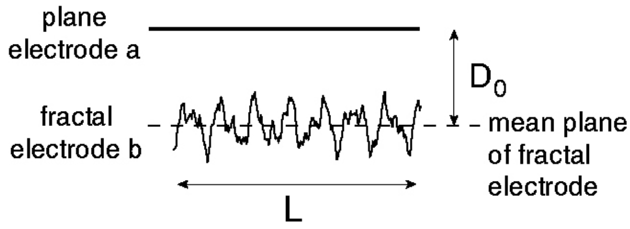

FIGURE 2. The geometry of the problem.

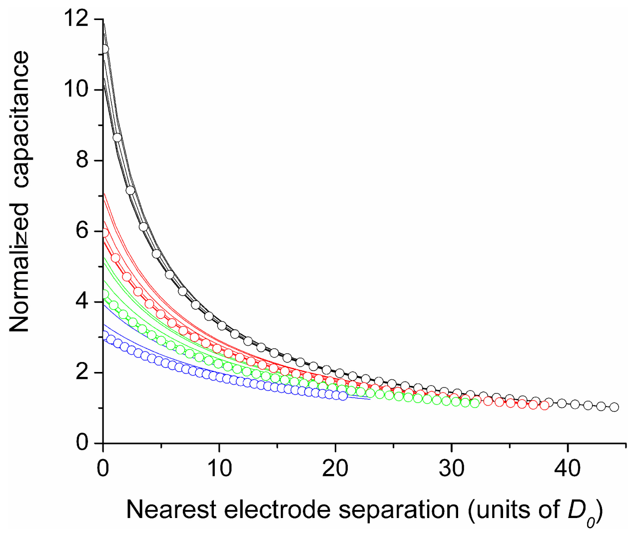

FIGURE 3. Graphs of normalized capacitance against nearest electrode separation for different values of σ and D. Black curves, $\sigma = 0.2D_0$; red curves, $\sigma = 0.4D_0$; green curves, $\sigma = 0.6D_0$; blue curves, $\sigma = 0.9D_0$. The values of D are, from the top curve to the bottom curve for each value of σ: 1.9, 1.8, 1.6, 1.4, 1.2 and 1.02. The value of b is 1.5. The open circles are the results for a Gaussian random rough surface with the same values of σ and a correlation length of $\tau = 1.0D_0$.

The equality of the capacitance calculated from the two electrodes is used as a check on the validity of the calculation. In the calculations presented here, the difference was typically less than 10^{-3}, although the roughest surface calculated showed a difference of the order of 10^{-2}.

3. Results and discussion

The results presented here were calculated by dividing a surface segment of length $\lambda_s = 30.0D_0$ into 512 points and assuming a periodic surface with 100 periods of these surface segments. The value of K_0 is given by

$$K_0 = \frac{2\pi}{\lambda_s/p},$$

where p controls the number of periods of the spatial frequency contributions in the surface segment. One aspect which is important to emphasize in the results presented here is that the values of capacitance are plotted against the nearest electrode separation, *i.e.* the smallest distance between a point on the rough surface and the planar probe electrode.

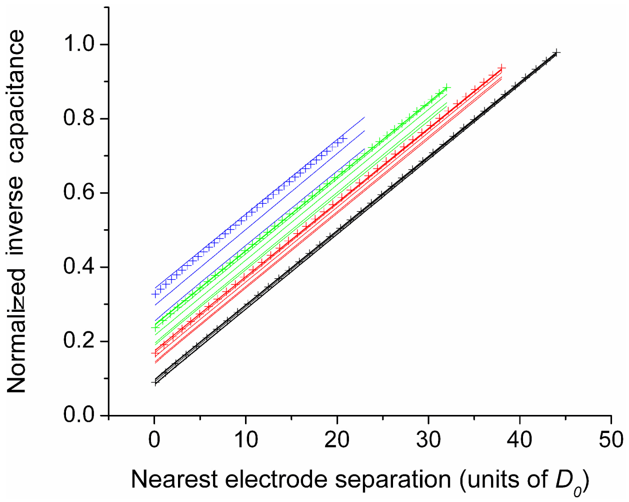

FIGURE 4. Graphs of inverse normalized capacitance against nearest electrode separation for the same data as in Fig. 2.

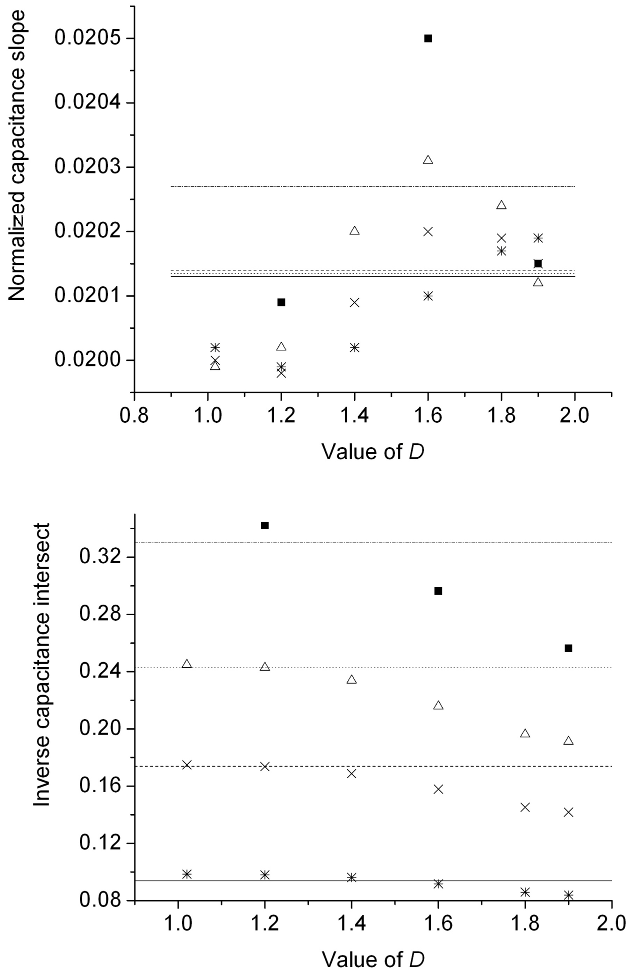

FIGURE 5. Graphs of the intersect point (lower) and the slope (upper) of the curves in Fig. 3 against the value of D. Filled squares, $\sigma = 0.9D_0$; open triangles, $\sigma = 0.6D_0$; crosses, $\sigma = 0.4D_0$; asterisks, $\sigma = 0.2D_0$. The lines are the results for a Gaussian rough surface with the values of σ given by: dashed and dotted line, $\sigma = 0.9D_0$; dotted line, $\sigma = 0.6D_0$; dashed line, $\sigma = 0.4D_0$; continuous line, $\sigma = 0.2D_0$.

This separation is measurable, whereas the distance between the average plane of the rough surface and the planar electrode is not [12]. The calculation for one value of the nearest electrode separation took approximately 15 minutes on a 167MHz SUN ULTRA 1 workstation.

Figure 3 shows the normalized capacitance values against the nearest electrode separation for fractal rough surfaces [Eq. (1)] with different values of the parameters σ and $D$and with the parameters b and p constant, and, for comparison, a similar curve for Gaussian rough surfaces with a constant correlation length τ_c and the same values for the width of the height probability distribution σ as the fractal surfaces. As in previous work [11], the Gaussian height distribution is cut at 3σ to limit the extent of the surface (a Gaussian distribution has a small but non-zero probability of producing a very high part of the surface which would mask the effect of the other parts of the surface on the capacitance). It can be seen that, for all cases shown, including the Gaussian surface case, the curves of the normalized capacitance versus nearest electrode separation have the same shape. However, the normalized capacitance is reduced as the parameter D is reduced or as σ is reduced.

The shape of the curves in Fig. 3 appear to follow a simple inverse relationship with the nearest electrode separation, so in Fig. 4 we plot the inverse of the normalized capacitance in Fig. 3 against nearest electrode separation. It can be seen that all the cases calculated here are straight lines in Fig. 4, showing that for all cases the normalized capacitance is an inverse function of the nearest electrode separation. Note that the curves in Fig. 4 should actually “dive down” to zero at the origin, that is, when the nearest electrode separation is zero the normalized capacitance is infinite, and thus its inverse is zero. It is rather surprising that the curves of the inverse ca-

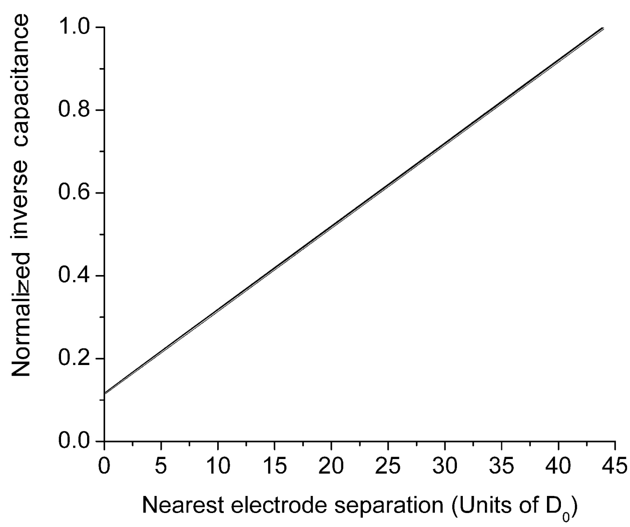

FIGURE 6. Graph of inverse normalized capacitance against nearest electrode separation for a band-limited fractal surface with $\sigma = 0.2D_0$ and a correlation length varying from 1.0 to 6.0. In this graph there are 7 different curves, which are indistinguishable.

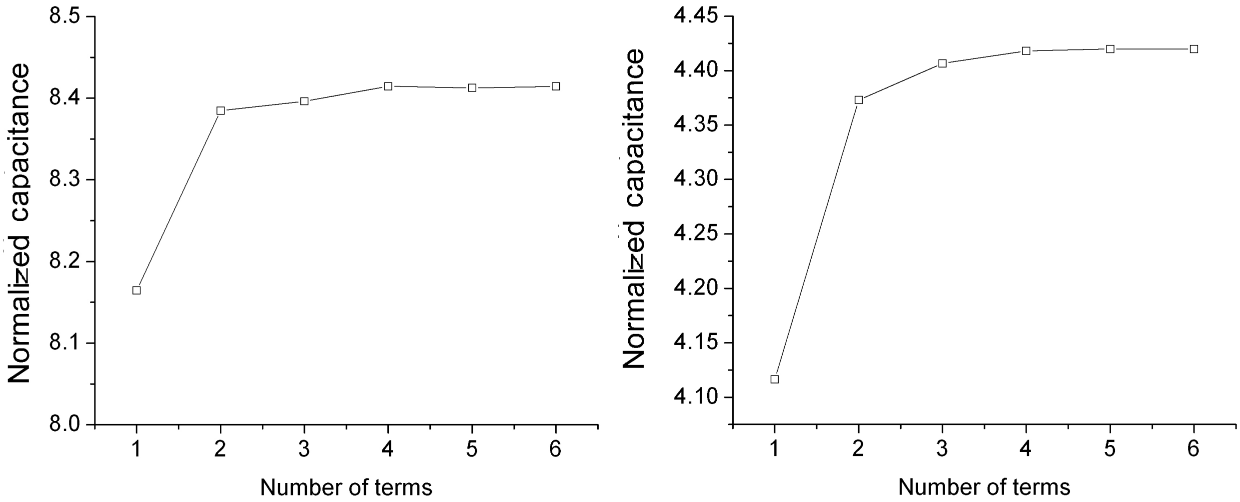

FIGURE 7. Graphs of normalized capacitance against the number, N, of spatial frequency components used in the surface generation for $\sigma = 0.2D_0$, left, and $\sigma = 0.4D_0$, right. The correlation distance for the cases shown is $\tau = 5D_0$.

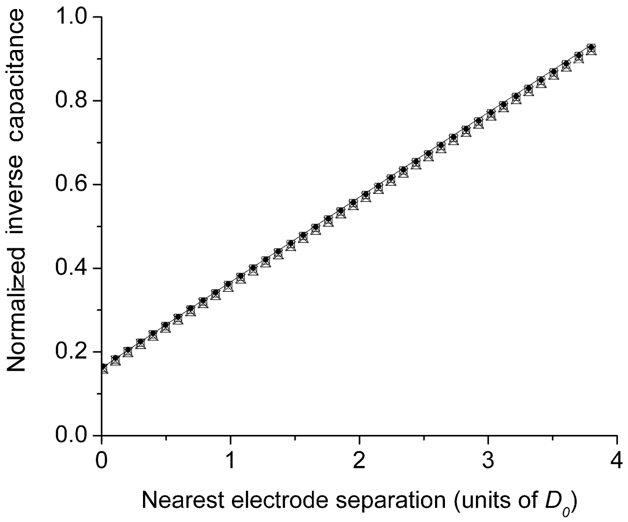

FIGURE 8. Graph of normalized capacitance against nearest electrode separation for different values of the parameter b for a band-limited fractal surface with $\sigma = 0.2D_0$ and $D = 1.5$. The crosses are for the case of $b = 1.02$; continuous line, $b = 1.2$; open squares, $b = 1.5$; filled circles, $b = 2.0$; and open triangles, $b = 2.5$.

pacitance remain linear down to a value of the nearest electrode separation of $0.01D_0$, which corresponds to the first point in the graphs. It is worth pointing out that taking a different separation parameter, *e.g.* the separation between the average plane of the rough electrode and the plane electrode, would give the same straight lines, with the same gradients, but shifted along the x-axis. For separations smaller than $0.01D_0$, the errors in the numerical method used here increase and the values of the capacitance calculated from the two electrodes differ by more than the value of 10^{-3} mentioned above. Figure 5 shows the variation of the slope and the intersection point on the y-axis of the different curves, *i.e.* fits the function $y = mx + c$, where y is the inverse capacitance, x is the nearest electrode separation, m is the slope of the data and c is the y-intercept. From this figure, we see that the slopes of the curves are independent of the parameters D and σ (note the small change in the vertical scale of the graph for the gradient m) whereas the intercept, c, does depend on the parameter D, as well as on the parameter σ.

Figure 6 shows the variation of the curve of the normalized capacitance versus the nearest electrode separation when the surface is stretched or shrunk in the horizontal direction. Here it is important to note that all cases had the same surface shape; this surface was only scaled in the horizontal direction. It can be seen that, as has been seen before for a randomly rough surface with Gaussian statistics, the capacitance obtained with a planar electrode is independent of the lateral structure for the fractal surface for the values of the correlation length shown here.

Figure 7 shows the variation of the normalized capacitance with the number of spatial frequency components N. From the graphs it can be seen that with 4 or more terms the capacitance is unchanged, i.e. the spatial frequencies in the surface shape for 4 or more terms have no effect on the measured capacitance. It can also be seen that the limit on the number of terms which affects the capacitance is independent of the standard deviation of the height. Although the value of N which affects the capacitance is small, from Figs. 3 and 4 it can be seen that the capacitance varies for cases with different parameters, so the fact that the surface is a band-limited fractal does affect the capacitance value.

Finally, Fig. 8 shows the variation of the inverse normalized capacitance against nearest electrode separation with parameter b, the spatial frequency scaling parameter. For the cases shown here, it can be seen that the normalized capacitance is independent of this parameter.

The results in Figs. 3-8 have a simple and appealing interpretation: the surface roughness on a flat electrode is equivalent to an artificial effective dielectric film on a flat conducting surface. To see this, let us recall that the capacitance of a parallel plate capacitor with a dielectric film covering one of its electrodes is given by

$$C = \frac{A\varepsilon_0}{d + \frac{h}{\varepsilon_r}}, \tag{8}$$

where A is the area of the capacitor,

$$\varepsilon_0 = 8.854 \times 10^{-12} C^2/N m^2$$

is the permittivity of free space, ε_r is the relative permittivity of the dielectric material, h is the thickness of the dielectric material, and d is the free space distance between the top of the dielectric layer and the second electrode. The normalized capacitance in this case is obtained by dividing Eq. (8) by $A\varepsilon_0$, and the inverse capacitance of this system is therefore

$$\frac{1}{C} = d + \frac{h}{\varepsilon_r} \tag{9}$$

i.e. the inverse capacitance is a linear function of the nearest electrode separation d, and the gradient of the linear dependence is independent of the parameters of the dielectric layer. The intersection point of the $1/C$ versus d line is the ratio h/ε_r, and so it does depend on the dielectric layer. This is the same situation as was found for the fractal surface case above: the gradient of the line is constant and the intersection point depends on the surface parameters.

Therefore our results indicate that the ratio of the effective coating thickness, h, and the effective dielectric constant ε_r depends mainly on the values of statistical parameters D and σ, and is nearly independent of the other parameters. The relationship between the rough surface parameters and the effective dielectric coating, for the specific case of very large nearest electrode separation compared to the height of the surface roughness, is studied in the Appendix.

This means that one could determine a relationship between the statistical parameters of the rough surface, D and σ, from the experimental measurement of the values of the capacitance between the rough surface and a parallel plane electrode for two or more values of the nearest electrode separation. The data from Fig. 4 can be used to produce a calibration curve as shown in Fig. 9, where the possible values of σ and D can be found from the intersection of the plane for the measured inverse capacitance intersect value with the curve of the inverse capacitance intersect value against σ and D. However, separating D and σgould require another independent measurement. Recently, it has been shown that it is, in principle, possible to determine the thickness and dielectric constant of a dielectric coating from two capacitive measurements using two electrodes of different shapes [14]. In this reference, it was shown that for two different electrodes, *e.g.* one plane and one circular, the dependence on the measured capacitance of the dielectric constant and the film thickness is different and that one measurement with each electrode is sufficient to separate these two parameters. In view of our finding that a fractal rough surface is equivalent to an effective dielectric film, it may be possible to use the technique proposed in Ref. 14 to obtain the values of an effective h and an effective ε_r and then separate the values of D and σu To obtain information on other statistical parameters of the rough surface, that is, b, K_0, and N, other independent measurements must be taken, *e.g.* optical scattering or microscopy measurements.

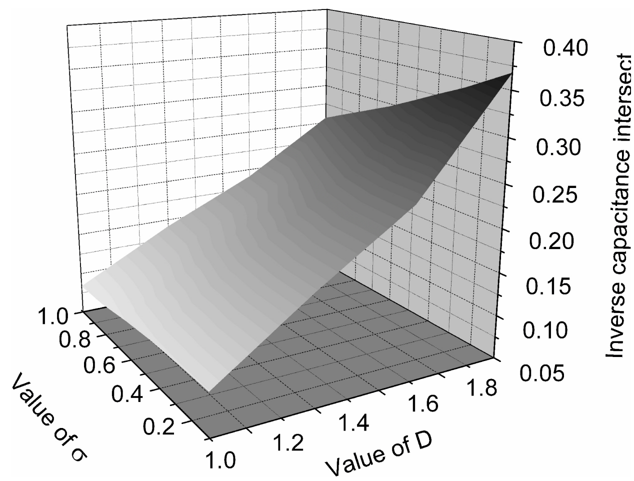

FIGURE 9. The calibration graph for the inverse capacitance intersect versus σ and D. The intersection of the plane for a measured value of the inverse capacitance with this curve gives the possible values of σ and D for the surface.

4. Conclusions

We have found that the inverse of the capacitance between a plane probe electrode and a band-limited fractal rough surface (us for a Gaussian random rough surface) is a linear function of the nearest electrode separation with the lines for different parameters having the same slope and different inverse normalized capacitance intersection values. There are 5 parameters which define the band-limited fractal rough surfaces used in this paper: σ which is the rms height, D $(1 < D < 2)$ which is the fractal dimension of the roughness, K_0 which is the fundamental spatial frequency, b $(b > 1)$ which is the spatial frequency scaling parameter, and N which is the number of spatial frequency components in the surface structure. Of these 5 parameters, the intersection point of the graph of the inverse capacitance value against nearest electrode separation depends on σ and D, as shown in Fig. 9. The slope of the inverse capacitance versus nearest electrode separation is independent of the surface parameters. This means that surface roughness with fractal statistics can be modeled by an artificial dielectric film with an effective thickness and an effective dielectric constant and that the ratio of the effective thickness and the effective dielectric constant is a function of σ and Donly. Some other, independent, measurement is required to separate these two parameters.

Appendix

There is a specific case in which the relation between the parameters of an effective thin dielectric layer over a conducting surface can be related to the shape of the rough surface in a simple way. For the case when the separation between the two electrodes is very large, $d \gg h$, in the case of the thin film, we have for the normalized capacitance

$$C = \frac{1}{d + \frac{h}{\varepsilon_r}} = \frac{1}{d}\left(1 + \frac{h}{\varepsilon_r d}\right)^{-1} \approx \frac{1}{d}\left(1 - \frac{h}{\varepsilon_r d}\right) = \frac{1}{d} - \frac{1}{\varepsilon_r}\frac{h}{d^2}, \qquad \text{(A.1)}$$

where we have used the binomial expansion and cut the series after the second term since $d \gg h$. The local height approximation for the normalized capacitance in a rough surface capacitor is [4,5]

$$C = \frac{1}{L}\int_L \frac{1}{d + h_{\max} - h(x)}\mathrm{d}x, \qquad \text{(A.2)}$$

where $d$is the nearest electrode separation and $h_{\max}$ is the maximum value of the surface height above the mean plane of the rough electrode, and the term $d{+}h_{\max}$ is the separation between the flat electrode and the mean plane of the rough electrode. Performing the binomial expansion as in (A.1), we obtain

$$\begin{aligned} C &= \frac{1}{L}\int_L \frac{1}{d}\left(1 + \frac{h_{\max} - h(x)}{d}\right)^{-1} dx \\ &\approx \frac{1}{L}\int_L \frac{1}{d}\left(1 - \frac{h_{\max} - h(x)}{d}\right) dx \\ &= \frac{1}{d} - \frac{1}{d^2}\left(Ah_{\max} - \frac{1}{L}\int_L h(x)\, dx\right). \end{aligned} \qquad \text{(A.3)}$$

Comparing Eqs. (A.1) and (A.3), it can be seen that the equivalent thin dielectric covering parameters are given by

$$\frac{h}{\varepsilon_r} = \left(h_{\max} - \frac{1}{L}\int_L h(x)\, dx\right) \qquad \text{(A.4)}$$

and, from Eq. (9) above, this parameter defines the intersection point of the inverse capacitance curves. This expression is true for any form of surface roughness, *i.e.* there will be an equivalent thin dielectric film for any shape of roughness. If the roughness is zero-mean (as is the case for the fractal surfaces), then the integral term in Eq. (A.4) is equal to zero and we have the equivalent thin dielectric covering parameters given by

$$\frac{h}{\varepsilon_r} = h_{\max}, \qquad \text{(A.5)}$$

i.e. the intersection point of the $1/C$ versus d curve depends only on the maximum value of the height of the rough surface. This means that, measuring with a plane electrode, it is not possible to extract the surface statistics for a zero-mean surface from the inverse capacitance intersection point, it is only possible to extract the maximum value of the surface height. In the case of the fractal surfaces, the maximum height of the surface depends on the value of σ, which gives the rms of the height variations, and on D, which defines the amplitudes of the different harmonic components. The other parameters should not affect the maximum height. This is the behavior found in the results above. If we choose a value of $h = 2\sigma$, then, from Eq. (A.5), we have

$$\varepsilon_r = \frac{2\sigma}{h_{\max}}, \qquad \text{(A.6)}$$

which could be used as a comparative parameter between surfaces with different statistics.

1. C.C. Williams, W.P.Hough, and S.A. Rishton, *App. Phys. Lett.* **55** (1989) 203.
2. C.P. Vlahacos, R.C. Black, S.M. Anlage, A. Amar, and F.C. Wellstood, *Appl. Phys. Lett.* **69** (1996) 3272.
3. S. Gómez-Moñivas, J.J. Saenz, R. Carminati, and J.J. Greffet, *Appl. Phys. Lett.* **76** (2000) 2955.
4. A. Garcia-Valenzuela, N.C. Bruce, and D. Kouznetsov, *Applied Physics Letters* **77** (2000) 2066.
5. N.C. Bruce, A. Garcia-Valenzuela, and D. Kouznetsov, *J. Phys D: Appl. Phys.* **32** (1999) 2692.
6. N.C. Bruce, A. Garcia -Valenzuela, and D. Kouznetsov, *J. Phys D: Appl. Phys.* **33** (2000) 2890.
7. S. Lányi, J. Török, and P.Rehurek, *J. Vac. Sci. Technol. B* **14** (1996) 892.
8. S. Lányi and M. Hruskovic, *J. Phys. D: Appl. Phys.* **36** (2003) 598.
9. S. Lányi and M Hruskovic, *Surface Science* **566** (2004) 880.
10. S. Lányi, *Ultramicroscopy* **103** (2005) 221.
11. N.C. Bruce and A Garcia-Valenzuela, *Meas. Sci. Tech.* **16** (2005) 669.
12. T.R. Thomas, *Rough Surfaces* 2^{nd} edition, (Imperial College Press, London, 1999) Sec. 8.4
13. D.L. Jaggard and X. Sun, *J. Opt. Soc. Am. A* **7** (1990) 1131.
14. A. Guadrrama-Santana, A. García-Valenzuela "Principles and methodology for the simultaneous determination of thickness and dielectric constant of coatings with capacitance measurements", *IEEE Transaction on Instrumentation and Measurement* (special issue on IMTC 05), accepted (2006).